

PRACTICAL EXPERIENCE WITH A DIGITAL ELECTROHYDRAULIC ACTUATOR

J. Tersteegen

(NASA-TT-F-15292) PRACTICAL EXPERIENCE  
WITH A DIGITAL ELECTROHYDRAULIC ACTUATOR  
(Kanner (Leo) Associates) : 39 p HC \$4.00

N74-15735

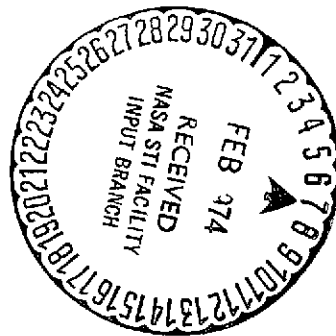
CSSL 01C

Unclass

G3/03

27527

Translation of "Praktische Erfahrungen mit einem digitalen  
elektro-hydraulischen Stellantrieb," Deutsche Forschungs-  
und Versuchsanstalt für Luft- und Raumfahrt,  
Report IB 153-73/26, 1973, 40 pages



1. Report No. NASA TT F-15,292	2. Government Accession No.	3. Recipient's Catalog No.	
4. Title and Subtitle PRACTICAL EXPERIENCE WITH A DIGITAL ELECTROHYDRAULIC ACTUATOR		5. Report Date February 1974	
		6. Performing Organization Code	
7. Author(s)  J. Tersteegen, Institut für Flugführung		8. Performing Organization Report No.	
		10. Work Unit No.	
9. Performing Organization Name and Address Leo Kanner Associates Redwood City, California 94063		11. Contract or Grant No. NASW-2481	
		13. Type of Report and Period Covered Translation	
12. Sponsoring Agency Name and Address National Aeronautics and Space Adminis- tration, Washington, D.C. 20546		14. Sponsoring Agency Code	
15. Supplementary Notes  Translation of "Praktische Erfahrungen mit einem digitalen elektro-hydraulischen Stellantrieb," Deutsche Forschungs- und Versuchsanstalt für Luft- und Raumfahrt, Report IB 153-73/26, 40 pages			
16. Abstract The basic feasibility of a digital electrohydraulic actuator has been demonstrated with the construction of a prototype. Implementation of this project required the development of electrohydraulic 3/2-way valves of high reliability and extremely short operating times. Satisfactory dynamic behavior on the part of the digital actuator is primarily determined by the accuracy of binary through-flow weighting. "Detrimental movement" (excess movement or movement in the wrong direction) due to inaccurate through-flow weighting or under loads should be avoidable if the output piston is locked until opposed low-level piston movements have been completed. The high-frequency detrimental movement of the digital actuator is filtered out when it is used as an anticipatory control instrument for a power amplifier to which it is connected.			
17. Key Words (Selected by Author(s))		18. Distribution Statement  Unclassified-Unlimited	
19. Security Classif. (of this report) Unclassified	20. Security Classif. (of this page) Unclassified	21. No. of Pages 34-39	22. Price 4.00

## Table of Contents

	<u>Page</u>
1. Introduction	1
2. The Design of the DEHA Prototype	2
2.1. 3/2-Way Valve	3
2.2. Locking Valve	7
2.3. Calibrated Orifices	10
2.4. Actuator Cylinder	14
3. Experimental Results with a DEHA Prototype	18
4. The DEHA As an Anticipatory Control Actuator	29
5. Summary	31

**PRECEDING PAGE BLANK NOT FILMED**

## Symbols

$A$	Flow cross section
$A_P$	Piston cross section
$A_R$	Piston rod cross section
$B$	Compressibility factor
$C$	Spring constant
$C_F$	Flow coefficient (throttle orifice)
$d_T$	Throttle diameter
$d_P$	Piston diameter
$d_R$	Piston rod diameter
$d_C$	Cylinder ID
$D_B$	Ball diameter
$D_N$	Nominal diameter
$D_S$	Valve seat diameter
$e$	Cylinder wall thickness
$E$	Modulus of elasticity
$F_S$	Spring force
$F_{stat}$	Static positioning force
$K$	Constant factor
$L_T$	Throttle length
$n$	Number of individual pistons
$N_{el}$	Electrical power to operate valves
$\Delta P$	Pressure change
$P_D$	Locking chamber ("differential chamber") pressure
$P_{cyl}$	Control pressure
$P_R$	Return pressure
$P_s$	System pressure
$Q$	Flow, throughput
$R_c$	Ohmic resistance of coil
$S_w$	Valve input signal
$\Delta Tr$	Resolution
$Tr$	Piston travel
$Tr_L$	Total piston travel during locked phase
$\Delta Tr_{SD}$	Piston travel due to deformation

$\Delta Tr_C$	Piston travel due to compressibility
$Tr_a$	Piston travel of power amplifier
$T_T$	Total valve operating time
$v$	Positioning velocity
$V_D$	Locking chamber volume
$\dot{V}_C$	Compressibility flow
$\dot{V}_{SD}$	Secondary deformation flow
$\rho$	Density

# PRACTICAL EXPERIENCE WITH A DIGITAL ELECTROHYDRAULIC ACTUATOR

Johannes Tersteegen,  
Institut für Flugführung

## 1. Introduction

/9\*

The practical development of a digital electrohydraulic actuator (called DEHA) in the following) was meant to demonstrate its serviceability and/or confirm the correctness of the theoretical considerations covered in the report "The Dynamic Behavior of a Digital Electrohydraulic Actuator" [1, 2]. In order to ensure that the information obtained with a laboratory model could be applied to a full-scale version, the requirement of a low weight:power ratio in aircraft equipment had to be taken into consideration in dimensioning the DEHA prototype. Output power was determined by using the DEHA both as an anticipatory control unit for an attached control-surface actuator with a mechanical input and for direct actuation of control surfaces on a test aircraft, in an integrated digital electrohydraulic control and regulating system.

The design of the DEHA prototype is based on the following technical data:

System pressure $P_s$	200 bar
Static positioning force $F_{stat}$	3140 N
Positioning velocity $v_{max}$	1 m·s <sup>-1</sup>
Resolution $\Delta Tr$	0.1 mm
Number of individual pistons $n$	9

---

\* Numbers in the margin indicate pagination in the foreign text.

## 2. The Design of the DEHA Prototype

As can be seen from [1, 2], inflow and outflow throttle orifices which are binary-stepped to correspond to the piston displacements are necessary for satisfactory transitional behavior of the DEHA without loads. An external load causes a change in the pressure drop across the orifices, however, and thus produces an error in transitional behavior, due to the resultant differences in piston travel time. Accurate transitional behavior should also be achieved under loads by means of the locking mechanism of the modified DEHA (Fig. 1).

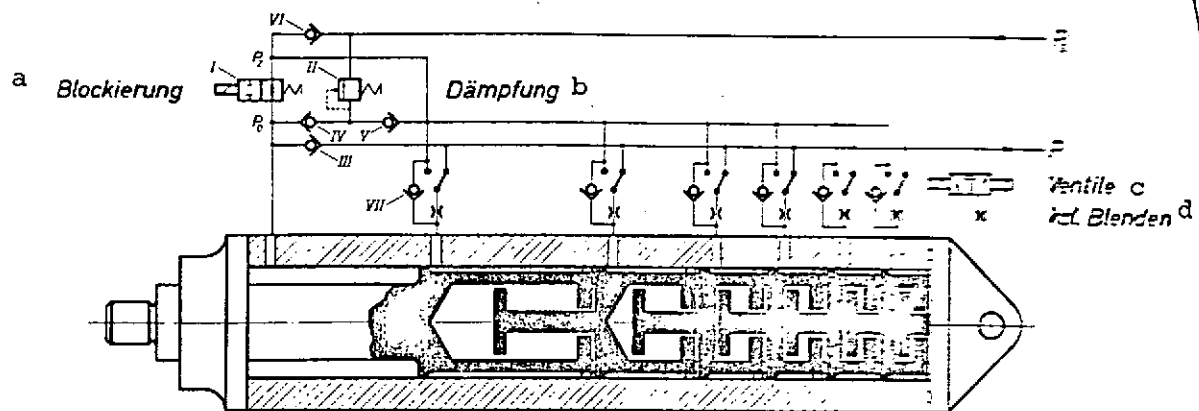


Fig. 1. Schematic design of a modified digital electrohydraulic actuator.

Key: a. Locking  
b. Damping  
c. Valves  
d. Calibrated orifices

The effects of external loading on transitional behavior can be simulated with an unloaded DEHA if binary-stepped inflow and outflow orifices are not employed. Consequently, the modified DEHA with the locking mechanism can be studied for serviceability /10 at low cost.

The relief valve and the check valves of the modified DEHA shown in Fig. 1 are necessary to achieve accurate transitional behavior in conjunction with the locking valve in the loaded DEHA, too. Since no actual external forces are applied in simulation, however, an additional simplification in constructing the DEHA can be made for the first laboratory trials by reducing the components, except for the locking valve (see Fig. 2). Only after positive results have been achieved using the locking valve will the modified DEHA, i.e. with the entire locking mechanism, be tested under external load in the second stage of testing.

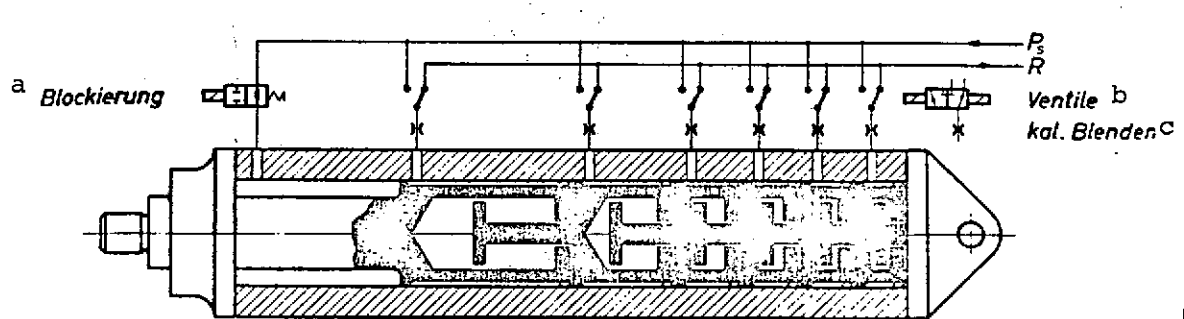


Fig. 2. Schematic design of a digital electro-hydraulic actuator with locking valve.

Key: a. Locking  
b. Valves  
c. Calibrated orifices

The design and the mode of functioning of the individual DEHA subassemblies are described in detail below.

### 2.1. 3/2-Way Valve

/11

The pistons are actuated with the aid of electrohydraulic 3/2-way valves. Since commercial valves do not satisfy the requirements for short operating times of less than 5 ms and high reliability, the development of suitable fast-acting valves



was begun in 1967 by the author of this report. The first positive results in experiments with a two-stage ball-type valve with hydraulic switching-position "memory" encouraged extensive research work in the field of switching elements and electro-hydraulic actuation. The results are published in the research report "Studies on Electrohydraulic Control Valves with Fluidic Ball Elements" by K.-H. Post [3].

Due to reliability requirements, it was necessary to dispense with the use of conventional plunger-type valves, which have a tendency toward hydraulic stoppage (jamming, seizing). The 3/2-way valve in the form of a seat-type valve with spherical operating elements was thus designed. Compared to plunger-type valves, seat-type valves offer the following advantages:

Hydraulic stoppage of the operating body is impossible. /12

The valve is insensitive to fouling, due to the self-cleaning action of flow at the valve seat.

The operating body forms a hermetic seal, even at extremely high pressures, without specially increased production precision.

The valve seat automatically readjusts itself as it is pounded by the operating element.

No friction shortens service life.

The high operating forces which occur in the direct actuation of the operating elements -- since static pressure forces are not compensated for -- necessarily result in a two-stage valve design beyond nominal diameter of about 2 mm. The use of additional plunger elements with sealing functions for static pressure compensation of the seat-type valve again

introduces valve elements with the disadvantage of the plunger. Since even at a nominal diameter of less than 2 mm the electrical retaining power to be applied by the electrohydraulic converter, e.g. a DC magnet, is too high, a hydraulic switching position "memory" device was provided for. This simultaneously satisfied the condition for the use of low-power pulse control, which also provides the advantage of low structural volume for the electrohydraulic converter.

The operating principle and the practical design of the hydraulic bistable three-way valve is shown in Fig. 3. In detail, the valve consists of two sets each of pushing DC magnets and anticipatory control, memory and control balls. A change in the position of the 3/2-way valve is triggered by a current pulse lasting about 3 ms to the appropriate magnet. The reversal of position will be described starting from position 1. A pulse to magnet 2 causes movement of the armature, which unseats anticipatory control ball 1 and seats anticipatory control ball 2 via a positive connection. This switching process causes a pressure drop in control line 1, subsequent reversal of memory ball 3, and thus a pressure buildup in control line  $X_2$ . With the pressure buildup in  $X_2$ , memory ball 4 is actuated and magnetically actuated anticipatory control balls 1 and 2 are held in position hydraulically. The pressure drop in  $X_1$  and pressure buildup in  $X_2$  also cause the reversal of control balls 5 and 6 into position 2.

Technical data on the 3/2-way valve shown in Fig. 3 are as follows: /14

External dimensions	60 x 40 x 20 mm
Ball diameter, first stage, $D_{B1}$	2 mm
Ball diameter, second stage, $D_{B2}$	4 mm
Nominal diameter $D_N$	2.5 mm
System pressure $P_s$	200 bar

*fin*

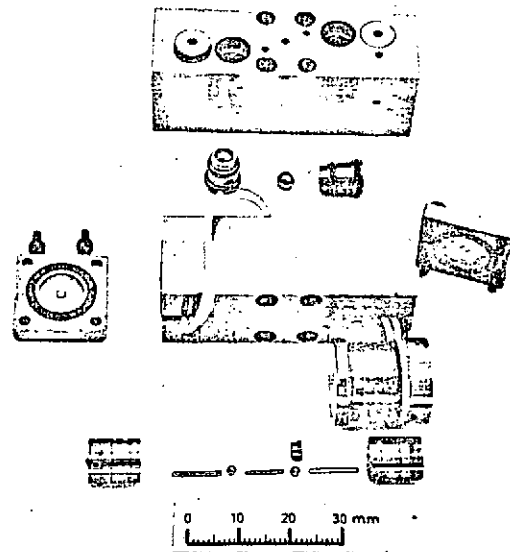
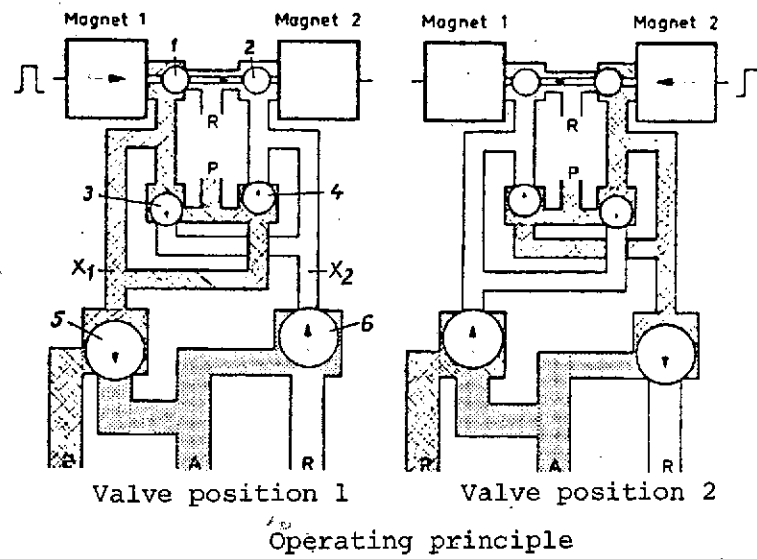


Fig. 3. Two-stage hydraulically bistable 3/2-way valve.

Input resistance of coils $R_c$ (220 windings, wire diameter 0.4 mm)	2.1 $\Omega$
Actuating power during switchover $N_{el}$	150 W
Switchover energy	0.4 Ws
Total operating time of valve $T_T$ (measured at the second stage at $P_s =$ = 200 bar)	2.5-3 ms

It was possible to reduce actuating power during switchover to 30 W and total operating time to 1 ms in a magnetically bistable two-stage three-way valve.

## 2.2. Locking Valve

The locking valve has the task of locking the highest-level pistons when the output variable of the DEHA is changed until lower-level piston movements in the opposite direction have been completed. "Detrimental" initial movements (excess movements or movements in the wrong direction) can only be avoided, however, if the locking valve closes absolutely tight during the locking phase. In addition, the requirements placed on the 3/2-way valve with regard to operating times and reliability also apply to the locking valve. Thus the locking valve was likewise put together from pure seat-type valve elements without plunger channels with a sealing function.

During part of the locking phase, a maximum pressure of

$$P_{Dmax} = 2P_s \quad (1)$$

develops in the locked chamber. If it is assumed that control pressure  $P_c$  is equal to supply pressure  $P_s$  in a ball-type valve (see Fig. 5), though, the condition for closure at a backpressure of  $P_D = 2P_s$  cannot be satisfied with a pure ball element. Thus /15 the locking valve was made of a spring-loaded ball element which

is actuated via an anticipatory control valve with a hydraulic position memory of the same design as in the 3/2-way valve. The operating principle of the locking valve is shown in Fig. 4.

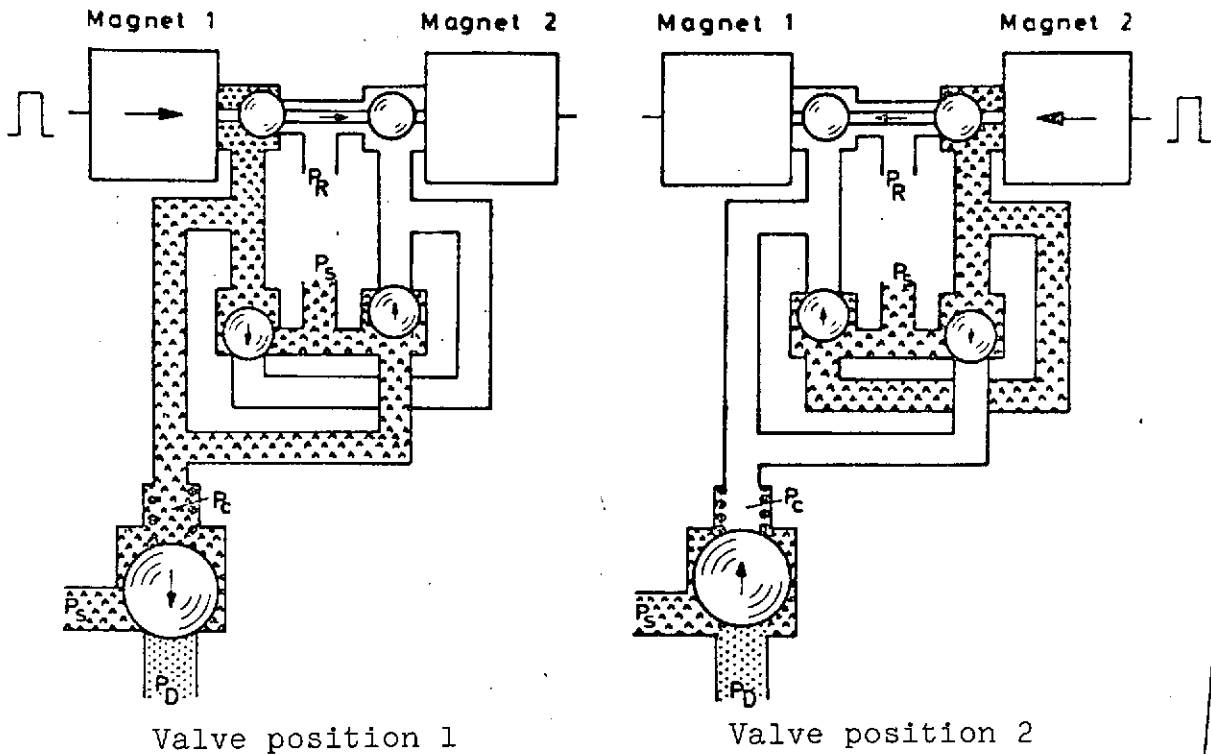


Fig. 4. Locking valve, operating principle.

With the notation used in Fig. 5, the following relations apply to operating conditions for the spring-loaded ball element:

a) Opening Condition

With  $P_C = 0$  and, in the most unfavorable case (DEHA without load after completion of opposed piston movements in the negative resultant direction), also  $P_D = 0$ , the opening condition is satisfied with

$$P_S (D_P^2 - D_S^2) \frac{\pi}{4} > F_S . \quad (2)$$

b) Locking Condition

If maximum differential chamber pressure is  $P_D = 2P_S$ , the locking condition reads

$$P_S D_S^2 \frac{\pi}{4} < F_S . \quad (3)$$

Additional design parameters for the locking valve can be derived from the operating conditions.

Substituting inequality (2) into (3) yields

$$\frac{D_P}{D_S} > \sqrt{2} . \quad (4)$$

Technical data on the locking valve are as follows:

External dimensions	22 x 61 x 70/20 x 20 x 60 mm	
Ball diameter, first stage, $D_{B1}$	2 mm	
Ball diameter, locking stage, $D_{BL}$	5 mm	
Nominal diameter $D_N$	2.5 mm	
System pressure $P_S$	100 bar	
Locking chamber pressure $P_D$	200 bar	
Spring force $F_S$	8.7 kp	
Spring constant $C$	0.5 kp/mm [1 kp = = 1 kg force]	
Input resistance of coils $R_C$ (220 windings, wire diameter 0.4 mm)	2.1 $\Omega$	<u>17</u>
Actuating power during switchover $N_{el}$	150 W	
Switchover energy	0.4 Ws	
Total operating time of valve $T_T$ (measured at second stage for $P_S =$ = 200 bar)	3 ms	

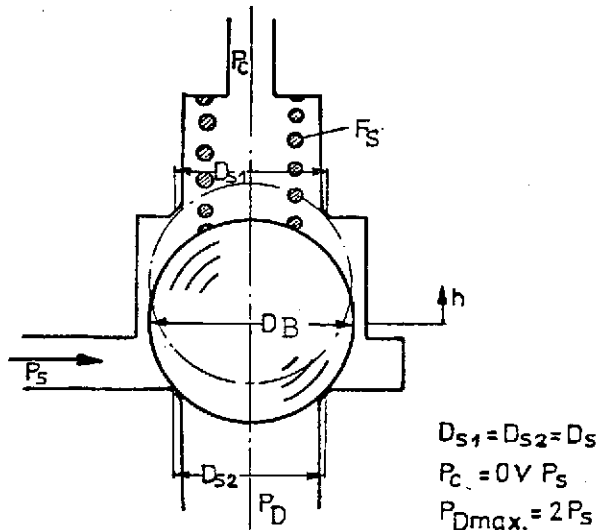


Fig. 5. Spring-loaded ball element.

### 2.3. Calibrated Orifices

Digital-to-analog conversion of the binary-coded signal into a dynamic component is accomplished via calibrated orifices by the evaluation of throughputs corresponding to the binary code. The transition velocity of the output piston is developed through summation -- via movement of the pistons -- of the flows evaluated this way in the

cylinder. The quality of transition behavior on the part of the unloaded DEHA and the loaded DEHA with locking mechanism when changes are made in the signal word in opposite directions is determined primarily by the precision of binary throughput weighting. Since weighting, once established, is not altered by external influences, e.g. a temperature difference at the orifices determining individual throughputs, an attempt must be made to maintain oil flow constancy in each case. Basically, although considerable difficulties arise, even small oil flows can be kept constant with a regulating system. The dynamic components required for this cause a reduction in reliability, however, due to the greater outlay. In order to avoid this disadvantage, an attempt was made to achieve an oil flow which was constant enough to meet requirements, using calibrated orifices.

Since a large number of articles [5-8] have already been published on orifice flows by many authors, the problem of keeping oil flows constant by means of an orifice will be covered only briefly in this paper, and experience gained in the design of a throttle will be reported. Largely unchanging flow coefficients

can be obtained even at low Reynolds numbers if the design of the throttle points (sharp leading edges, maximum possible ratio between oncoming-flow cross section and throttle cross section) results in turbulent flow. Under these conditions, it is possible to calculate throttle cross sections approximately with /18 the orifice equation

$$Q = C_F \cdot A \cdot \sqrt{\frac{2 \cdot \Delta P}{\rho}} \quad (5)$$

where  $Q$  = Flow through orifice  
 $C_F$  = Flow coefficient  
 $A$  = Flow cross section  
 $\Delta P$  = Pressure drop across throttle point  
 $\rho$  = Density.

Flow coefficient  $C_F$  is determined experimentally with actual system orifices in order to take real operating conditions into consideration. The values given in the literature are unusable in this respect, since they vary over a wide range (up to 20%), depending upon the orifice shape and measurement precision employed and upon experimental conditions. In order to make flow coefficient  $C_F$  almost independent of oil temperature variation (viscosity variation), of supply pressure  $P_s$ , of pressure downstream from the throttle and of pressure drop  $\Delta P$ , the ratio of throttle length  $L_T$  to throttle point diameter  $d_T$  should be  $\leq 1/7$  if possible. Production-engineering aspects and strength considerations establish limitations here, however -- no permanent orifice deformation may occur even at high pressure differentials. Through-flow is only slightly dependent upon the specified influencing parameters even for values of  $L_T/d_T \leq 9/10$ . The effect of viscosity on through-flow can be further reduced by decreasing the pressure drop at the throttle point. For a given supply pressure, this calls for several orifices arranged in succession, with an increased flow cross section. The danger of stoppage in case of oil contamination is simultaneously reduced



with the increase in flow cross section. The application of a throttle point consisting of several orifices arranged in series offers the additional advantage that through-flow can be adjusted over a wide range by varying the number of cross sections of the orifices used. The problem associated with the production of binary-weighted flow orifices is also thereby avoided, since not every desired orifice cross section can be produced, due to the large steps between drill diameters. Spark-erosion methods require a considerably increased outlay.

In designing a throttle point consisting of several orifices arranged in series, care must be taken to see that the flow orifices are not aligned, in order to prevent the formation of partially laminary flow. The eccentric hole in an orifice piece /19 (see Fig. 6) should always be diametrically opposed to an equivalent orifice which follows it, to eliminate ambiguity. Eccentricity should amount to at least  $1/2$  hole diameter. Tests have shown that through-flow can be affected by reducing the distance between holes in two successive orifices (by rotating the orifice pieces relative to one another), since inflow conditions in the fluid medium change at each orifice. This effect can also generally be used to adjust to a certain through-flow. The orifices must then be fixed relative to one another, however, so that calibration of the throttle, once undertaken, is not lost during operation or in the event of later disassembly.

It can be seen from the descriptions in the preceding sections that the medium flows through the throttle in both directions, depending upon the position of the  $3/2$ -way valve. Satisfactory transitional behavior of the unloaded DEHA results if the same flow occurs for equal pressure drops across the throttle in both directions. Through-flow which is independent of direction occurs only under symmetrical flow conditions, however. These require geometrically equivalent inlet and

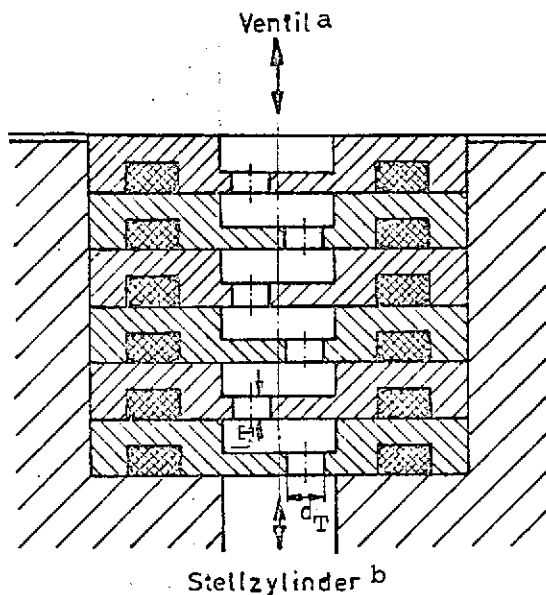


Fig. 6. Throttle valve with several calibrated orifices.

Key: a. Valve  
b. Actuator cylinder

outlet openings and equivalent oncoming-flow openings. Since, in practice, it is not possible to produce absolutely sharp leading edges, and the edge radii which are thus presented in the two directions are usually different, the through-flows must be matched, if required in the calibration of orifices, by slightly beveling the leading edges. Tests have indicated that chamfering the "leading edge" located downstream increases flow coefficient  $C_F$  for this flow direction, whereas such a step has only a slight effect

upon flow in the other direction.

#### Technical Data

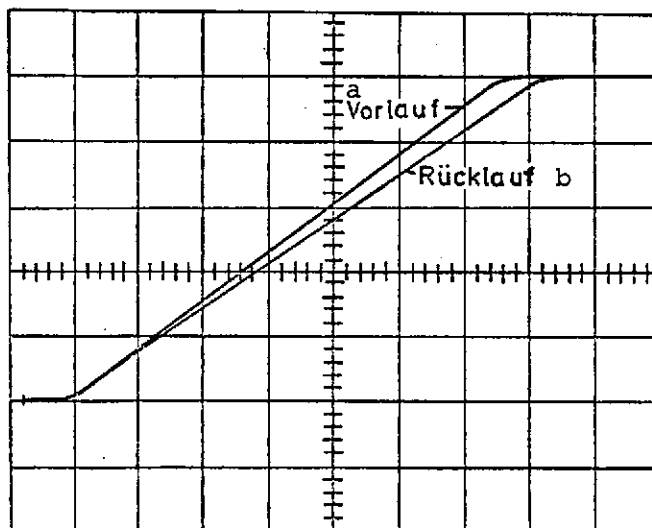
Each throttle consists of six orifices arranged in series, with theoretically determined hole diameters of

$d_0 = 0,11 \text{ mm}$	$d_3 = 0,32 \text{ mm}$	$d_6 = 0,92 \text{ mm}$
$d_1 = 0,16 \text{ mm}$	$d_4 = 0,46 \text{ mm}$	$d_7 = 1,30 \text{ mm}$
$d_2 = 0,23 \text{ mm}$	$d_5 = 0,65 \text{ mm}$	$d_8 = 1,84 \text{ mm}$

[Note: Commas in numerals are equivalent to decimal points.]

Throttle through-flow length  $L_T$  is graduated from 0.3 mm at  $d_0$  to 0.85 mm at  $d_8$ . The orifice pieces (outside diameter 10 mm, thickness 1.5 mm) were mounted in a distributor panel between the valves and the cylinder.

Orifice calibration was checked in the assembled DEHA prototype by measuring piston-rod velocity as an oscillograph plot of piston-rod travel versus time. Satisfactory transitional DEHA behavior is only obtained if the travel/time diagrams for all piston displacements in both directions are geometrically similar. This requirement was tested by first plotting the travel/time curves for both piston directions on an image of a cathode-ray storage oscilloscope (CO). The requirements were satisfied if piston return could be made congruent with piston advance by reversing its sign on the CO. In the example shown (see Fig. 7), a deviation still exists in the travel/time curves for the two piston movements. In order to obtain a comparison of the travel/time curves for all piston displacements, the scale for piston travels was chosen to correspond to the binary code, so all displacements achieve equal image height in the oscillogram.



Time scale 10 ms/Div.

System pressure  $P_s$  98 bar

Fig. 7. Travel/time curves for piston displacement  $2^4 = 1.6$  mm. Piston return has the same direction on the CO as piston advance, due to the reversal of sign.

Key: a. Advance; b. Return

## 2.4. Actuator Cylinder /21

The d-a conversion of the binary-coded signal in a static component is accomplished in the actuator cylinder through weighting of the individual cylinder displacements to correspond to the binary code. Output variable  $Tr$  is generated by the summation of piston displacements weighted in this manner.

The design of the pistons, arranged in series and made to engage one another, can be seen in Fig. 8. The assembly was produced by Liebherr-Aero Technik GmbH, Lindenberg, under contract to the DFVLR. The manner in which the cylinders engage one another was chosen, in particular, on the basis of strength considerations, since the devices by which the pistons engage one another can be alternately subjected in the most unfavorable case to a maximum force of  $P_s \cdot A_p$  during the locking phase.

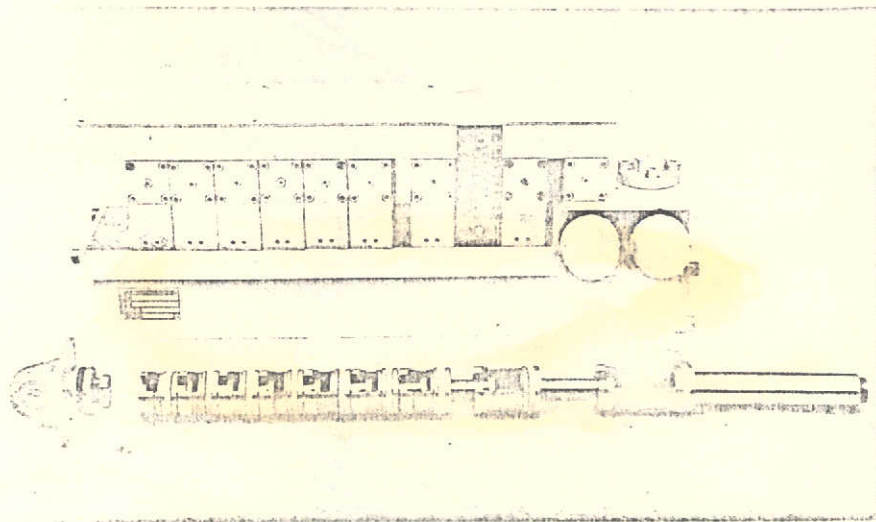


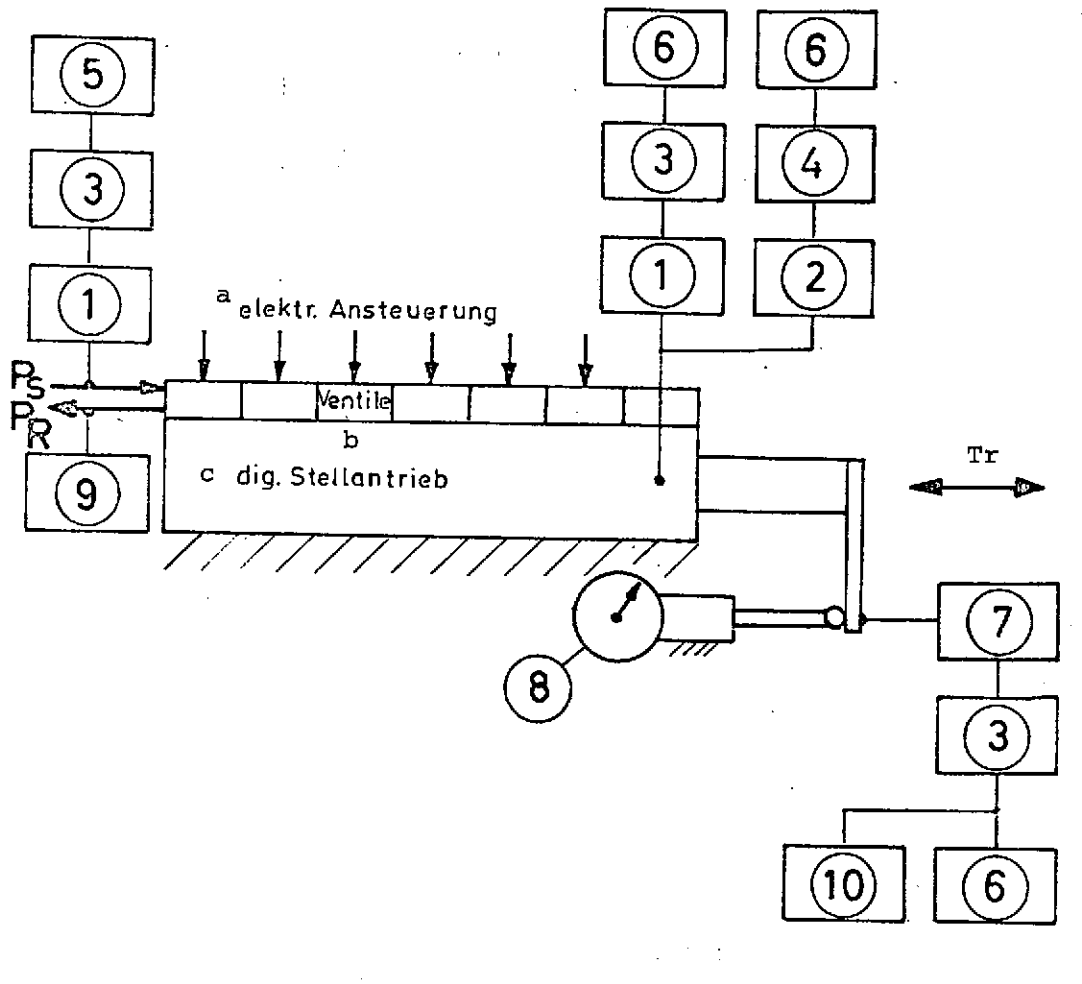
Fig. 8. Actuator cylinder and engaged pistons.

To be sure, this design does not make it possible to observe /22 the required tolerance in individual piston travel of  $\pm 0.01$  mm during production. These problems should be eliminated with another design now being produced, in which the engaging devices consist only of turned parts. Aside from travel, the assembled length of the actuator cylinder is determined primarily by the length of the individual pistons, since their channel length must be approximately equal to piston diameter, due to the danger of canting. In the actuator cylinder which was built, this means a channel length of about 20 mm even for the lowest-level piston, with a travel of 0.1 mm. High requirements were placed on the

sealing elements of the pistons. Unsuitable seals cause irregularities in the transitional behavior of the DEHA without the locking mechanism, due to leakage between the piston chambers, due to piston chamber volumes which change as a result of deformation of the sealing element or shifting of the sealing element in the ring groove during pressure changes, and due to excessive frictional forces. Variable leakage -- a function of the positions into which the neighboring pistons have been switched -- and variation of the piston chamber volume are equivalent, in their effects upon transitional behavior, to an inconstant flow through the calibrated orifice. Frictional force -- a function of the number of pistons to be moved -- corresponds to the case of a load of constant force on the DEHA. In the DEHA with a locking mechanism, unsuitable seals for the locking chamber result, due to leakage and to deformation and shifting of the sealing elements in the ring groove, in displacement of the locked output piston and thus likewise in irregular transitional behavior. After a variety of tests, Glyd rings were finally used as seals. The pistons were given a Rilsan finish in order to reduce friction between the pistons, made of steel, and the cylinder, made of aluminum. /23

#### Technical Data

Dimensions	35 x 35 x 299 mm
System pressure $P_s$	200 bar
Piston diameter $d_p$	20.34 mm
Piston rod diameter $d_R$	14.29 mm
Deviation in area ratio $A_R/A_P$ relative to $A_p$	1.2%
Resolution	0.1 mm
Binary stepping of piston travel from 0.1 to 25.6 mm with a tolerance of ...	$\pm 0.04$ mm
Total travel $Tr$	51.1 mm



1. Pressure pickup, Hottinger P3M/500 kp/cm<sup>2</sup>
2. Pressure pickup, Kistler 701 HX1/600 at [1 at = 1 technical atmosphere = 1 kg/cm<sup>2</sup>]
3. Carrier frequency amplifier, Hottinger KWS/3-5
4. Charge amplifier, Kistler
5. Digital voltmeter, four-place readout
6. Cathode-ray storage oscilloscope
7. Inductive displacement pickup, Hottinger, 50 mm
8. Extension meter, dial precision 10  $\mu$ m
9. Temperature measurement
10. X-Y recorder
- a. Electronic triggering
- b. Valves
- c. Digital actuator

Fig. 9. Schematic of the test setup.

Absolute static positioning precision	$\pm 0.15$ mm
referred to total travel Tr	$\pm 0.3\%$
Number of possible positions	512

The piston travel deviations from the desired values were measured using a gauge with a dial precision of 10  $\mu\text{m}$ .

### 3. Experimental Results With a DEHA Prototype

/25

Results on the dynamic behavior of the DEHA prototype will be reported in summarized form in this part of the paper. Results of experiments on the static behavior of the actuator can be found in the last section, in the description of the assembly. The experimental studies were carried out with the test setup shown in Fig. 9.

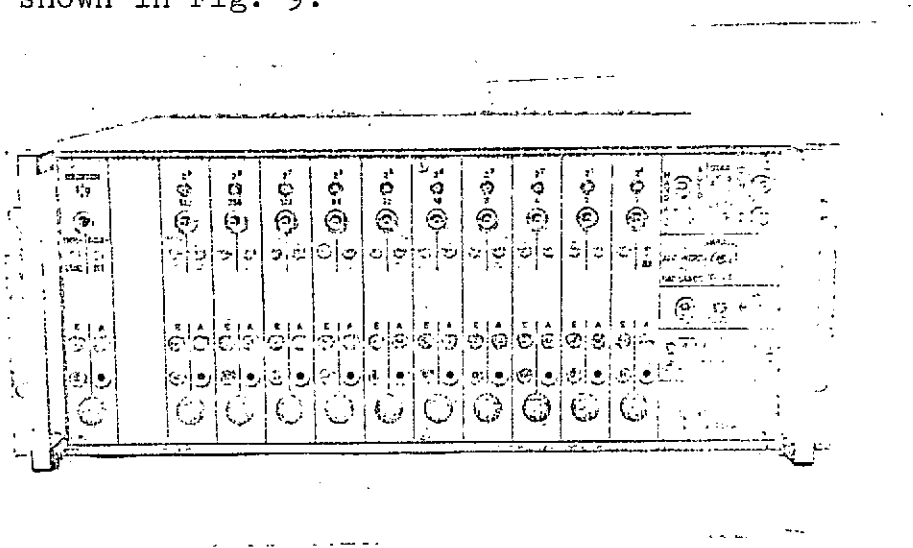


Fig. 10. Electronic triggering unit.

The valves were triggered with an electronic unit (see Fig. 10) developed in Institute L of the DFVLR by Ing. (grad.) R. Dombrowsky. The analog signal coming from a waveform generator or a signal presented in decadic form with a manual input instrument is converted into a digital, binary-coded

/26

signal in the triggering unit, scanned at regular intervals, and sent on to the 3/2-way valves and the locking valve in a certain sequence. The locking valve is locked only in a case of opposing changes in the signal word. The valves can also be picked individually by means of additional switches in the triggering unit. In order to achieve an optimum triggering of valves -- since a sound evaluation of the dynamic behavior of the DEHA is only possible under this condition -- additional adjustment provisions were built into the triggering instrument. Thus pulse length can be adjusted to the valve operating times. Since the switching pulses for the 3/2-way valves must appear later than the pulse for the locking valve after the instant of scanning, an initial delay can also be adjusted for simultaneously for all valves, taking the pulse length for the locking valve into consideration. Dead times of various lengths in the valve switching process can be matched to one another by introducing an additional delay for the instant at which the individual pulse is cut in. Finally, the possibility exists for selecting locking time for adaptation to piston travel time. The various possible settings are plotted in the pulse schedule, Fig. 11.

After the travel/time curves for the individual pistons were plotted on a storage CO and the results were evaluated, the following settings were selected for the triggering instrument for experiments on the dynamic behavior of the DEHA:

/27

Control valve:	Pulse length	3 ms
	Common initial delay	4 ms
	Pulse delay	0 ms
Locking valve:	Pulse length	3 ms
	Locking time	60 ms

Since a pressure of  $P_D = 2P_S$  can occur in the locking chamber during the locking phase, but the actuator cylinder is designed for an operating pressure of only 200 bar, almost all



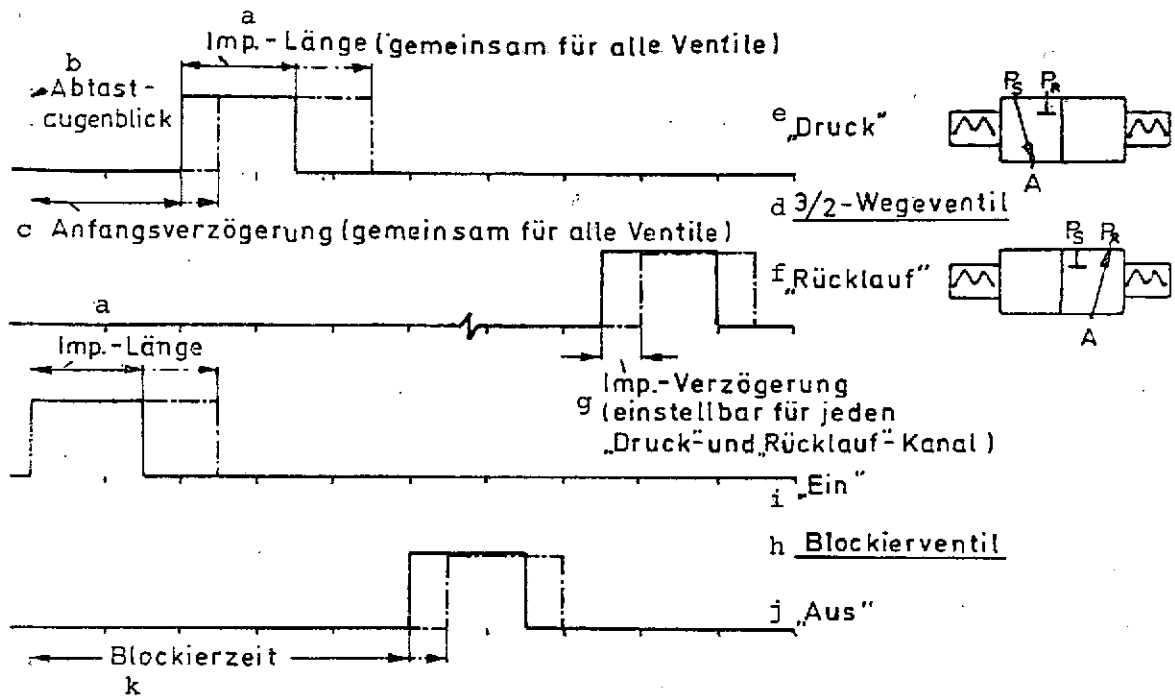
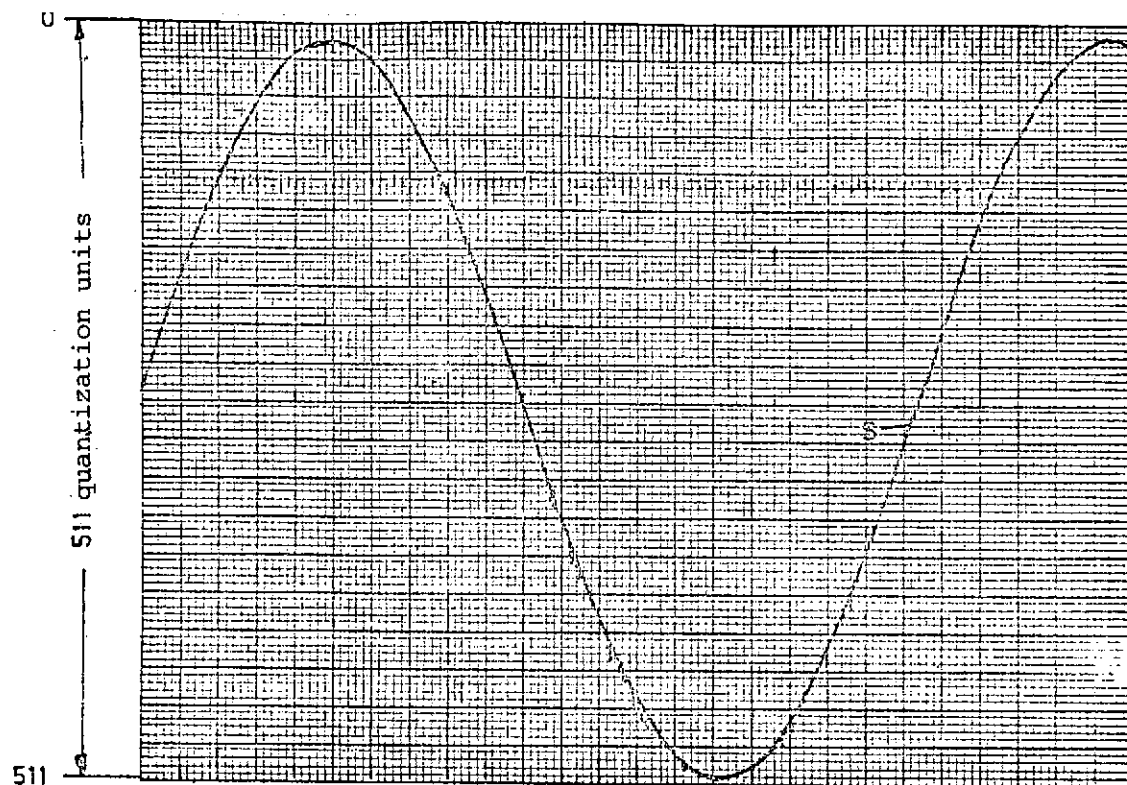


Fig. 11. Pulse schedule for triggering the DEHA.

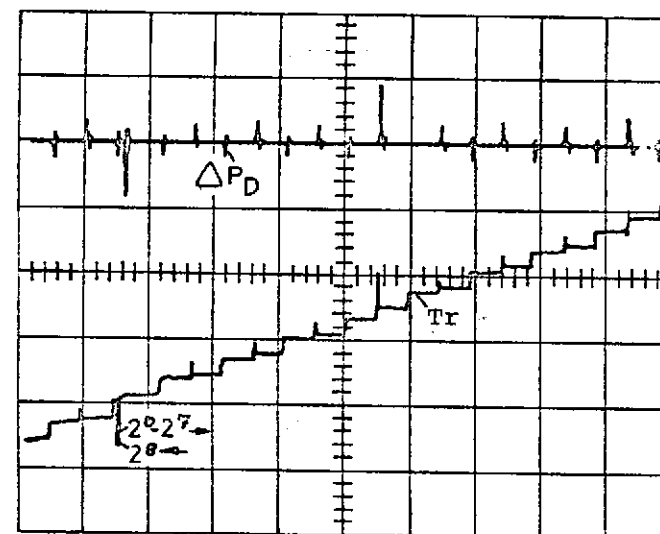
- Key:
- a. Pulse length (common to all valves)
  - b. Instant of scanning
  - c. Initial delay (common to all valves)
  - d. 3/2-way valve
  - e. Pressure
  - f. Return
  - g. Pulse delay (adjustable for each "pressure" and "return" channel)
  - h. Locking valve
  - i. On
  - j. Off
  - k. Locking time

tests were carried out with a system pressure of  $P_s = 98$  bar. It was possible to keep operating temperature constant at  $26^\circ\text{C} \pm 1^\circ\text{C}$  during all of the measurements. The piston travel times were calibrated to about 50 ms under these operating conditions.

The resultant motion of the output piston is plotted in Fig. 12. The travel/time curve in the left graph is the



Time scale 10 s/Div.  $s = Tr$   
 Frequency 0,01 Hz  
 Cycle frequency 6 Hz  
 System pressure 108 bar



Time scale 1 s/Div.  
 Pressure scale 98 bar/Div.  
 Step width 0,1 mm  
 System pressure 98 bar

Fig. 12. Resultant movement of the DEHA output piston.

result of a sine function and, in the enlarged section, that of a ramp function as the input variable. The trials were executed with calibrated orifices and a locking valve. It can be seen just from these first experimental results that no absolute locking of the output piston has occurred (a noise signal is superimposed on the sinusoidal oscillation). The weighting errors which still exist in the through-flows are manifested in the output as excessive movements or movements in the wrong direction in the output when opposed changes occur in the signal word. The reason for the presence of weighting errors in the through-flows must be sought in calibration on the storage CO, which cannot be carried out with great precision (image scale is too small). Due to the mode of representation, it is also almost impossible to analyze the relative size of weighting error. A check should be made as to whether better results could be achieved by using a light-spot line recorder. It should be mentioned here that a check of orifice calibration by means of a through-flow measurement only promises more accurate results if the weighting error in piston displacements and the deviations in the ratio of piston to piston rod cross section from 2:1 can be neglected.

The reason for incomplete locking of the output piston was pursued in additional tests, which were conducted in compliance with the conditions given in Section 2. First, it was possible to demonstrate that the locking valve closed off the locking chamber completely when it was cut in. In addition, the absence of air in the locking chamber was guaranteed by suitable evacuation.

The effect of elasticity and/or compressibility upon locking can be seen unequivocally in the various trials (see Figs. 13 and 14). The curves also indicate that leakage from the locking chamber to the neighboring chamber cavity can be

ruled out on the basis of the pressure differential. This was to be expected, since a leakage flow could not have the indicated effects, due to the short operating times.

During the locking phase, the volume of oil enclosed in the locking chamber is compressed when a signal change for positive resultant movements occurs and is decompressed for negative resultant movements. The so-called compressibility flow  $\dot{V}_C$  which results from this is defined as follows in accordance with [4]:

$$\dot{V}_C = \frac{V_D}{B} \dot{P}_D$$

$V_D$  = volume of locking chamber  
 $B$  = compressibility factor  
 $\dot{P}_D$  = Pressure change in locking chamber.

(6)

Piston displacement  $\dot{Tr}_C$  due to compressibility is

$$\dot{Tr}_C = \frac{\dot{V}_C}{\frac{A_P}{2}}$$
(7)

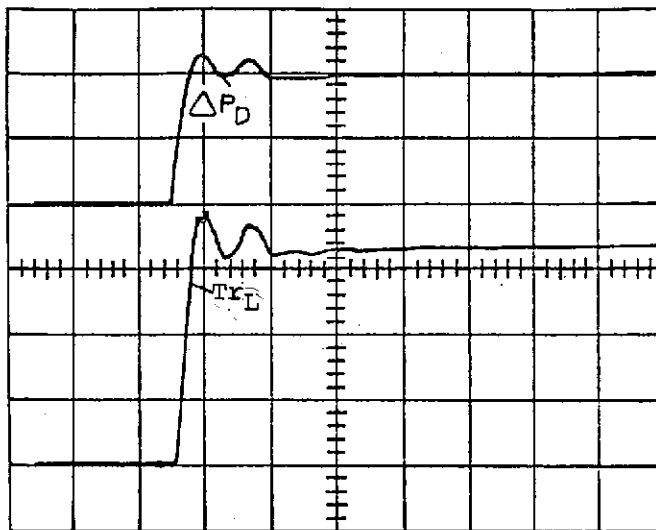
By substituting equation (6) into equation (7) we obtain the relative change in total piston displacement  $Tr_L$  during the locking phase:

$$\frac{\Delta Tr_C}{Tr_L} = \frac{V_D \cdot \Delta P_D \cdot 2}{B \cdot A_P \cdot Tr_L}$$

$\Delta P_D$  = absolute value of pressure change in locking chamber  
 $A_P/2$  = reduced piston area.

(8)

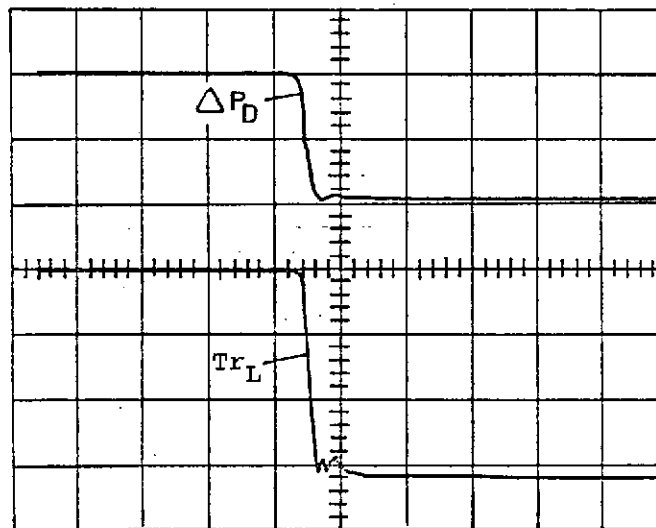
In the trial shown in the upper part of Fig. 14, the volume of oil enclosed in the locking chamber is  $V_D = 5.21 \text{ cm}^3$ , piston area is  $A_P/2 = 1.64 \text{ cm}^2$ , measured total piston displacement is  $Tr_L^* = 0.33 \text{ mm}$ , and the pressure rise is about 98 bar.



$2^0, 2^1$  and  $2^8$  retracted

$2^2$  to  $2^7$  extended

Plot:  $2^8$  is activated



$2^0$  to  $2^7$  retracted

$2^8$  extended

Plot:  $2^8$  is inactivated

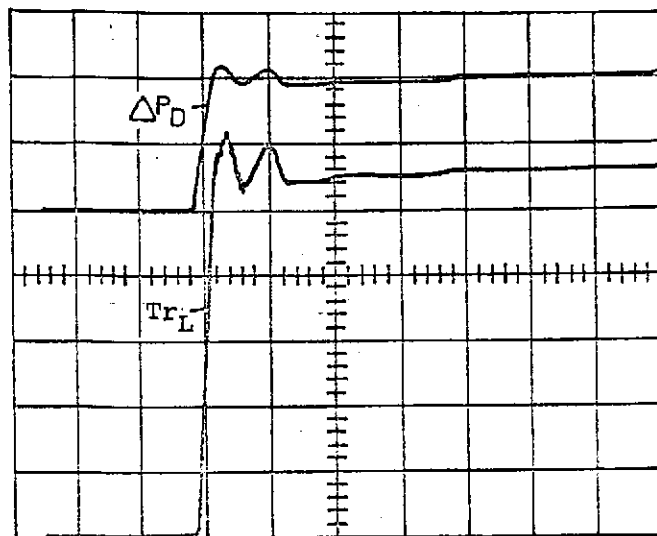
Time scale: 10 ms/Div.

Pressure scale: 49 bar/Div.

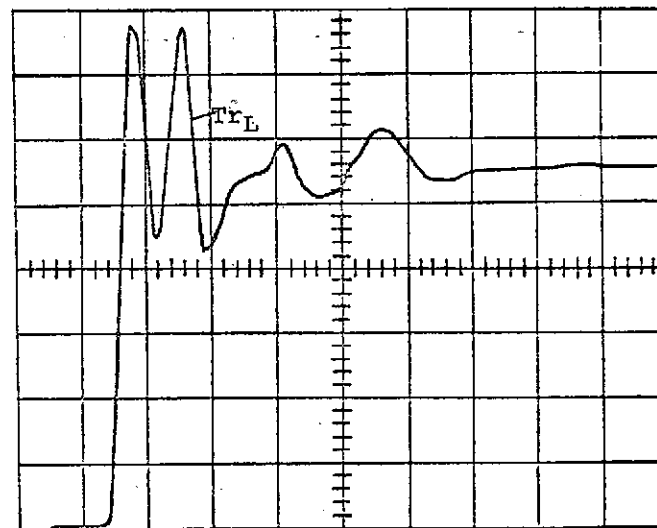
Travel scale: 0,1 mm/Div.

System pressure: 98 bar

Fig. 13. Piston displacement  $Tr_L$  during the locked phase.



2<sup>0</sup> to 2<sup>8</sup> retracted  
 Plot: 2<sup>8</sup> is activated



2<sup>0</sup> to 2<sup>8</sup> retracted  
 Plot: 2<sup>2</sup> to 2<sup>8</sup> are activated

Time scale: 10 ms/Div.  
 Pressure scale: 49 bar/Div.  
 Travel scale: 0,1 mm/Div.  
 System pressure: 98 bar

Fig. 14. Piston displacement  $Tr_L$  during the locked phase.

Using an assumed compressibility  $B = 12,000$  bar for the hydraulic oil, MIL-H-6083 (Aeroshell Fluid 7), we calculate piston displacement  $\Delta Tr_L$  to be  $0.79 Tr_L^*$ . If we also take into consideration the error of about  $0.06 Tr_L^*$  (determined experimentally) which results from the relative volume change due to the quartz crystal pressure pickup connected to the locking chamber, we obtain a piston displacement  $\Delta Tr_C$  due to compressibility of about  $0.84 Tr_C$ . /32

As the result of pressure differentials in the locking chamber, material deformation occurs in the actuator cylinder which results in a so-called secondary deformation flow  $\dot{V}_{SD}$ . In the elastic range,

$$\dot{V}_{SD} = K \cdot \dot{P}_D \quad (9)$$

The factor  $K$  is a function of the design of the actuator cylinder and of the material. If we assume rigid cylinder caps and pistons and consider a thin-walled cylindrical vessel -- which permits a simpler computation which nevertheless is sufficient for an estimate -- we can, according to [4], write  $K$  as follows:

$$K = \frac{5}{2} \frac{V_D \cdot d_C}{E \cdot 2 \cdot e} \quad \begin{array}{l} V_D = \text{volume of locking chamber} \\ E = \text{modulus of elasticity} \\ d_C = \text{cylinder ID} \\ e = \text{cylinder wall thickness.} \end{array} \quad (10)$$

For secondary deformation flow  $\dot{V}$ , we can then write

$$\dot{V}_{SD} = \frac{5}{4} \frac{V_D \cdot d_C}{E \cdot e} \dot{P}_D \quad (11)$$

Piston displacement  $\dot{Tr}_{SD}$  resulting from deformation flow is

$$\dot{Tr}_{SD} = \frac{\dot{V}_{SD}}{\frac{A_P}{2}} \quad (12)$$

By substituting equation (11) into equation (12) we obtain the relative change in total piston displacement  $Tr_L$  during the locked phase as

$$\frac{\Delta Tr_{SD}}{Tr_L} = \frac{5 \cdot \frac{V_d \cdot d \cdot C \cdot \Delta P_D}{2 \cdot E \cdot e \cdot A_P \cdot Tr_L}}{Tr_L} \quad (13)$$

Using the experimental data from the last section and a cylinder ID of 20.3 mm, a cylinder wall thickness of 7.5 mm and a modulus of elasticity of  $7.1 \cdot 10^6$  N/cm<sup>2</sup>, we calculate piston displacement  $\Delta Tr_{SD}$  to be about 0.05  $Tr_L$ .

733

An additional secondary deformation flow which apparently causes the remaining piston displacement of 0.11  $Tr_L$  during the locked phase is produced during the pressure rise or drop by the elasticity and mobility of the seals in their grooves.

The analysis which was performed made it possible to determine the cause of the faulty behavior of the DEHA and the part played by the influencing parameters in total displacement of the output piston during the locked phase. The absolute value of error in movement varies, as can be seen from equations (8) and (13), proportionally with respect to locking chamber volume and with travel and pressure change in the locking chamber, due to compressibility and material deformation. The portion due to the seals can be considered approximately constant, since it does not change appreciably with pressure. If it is assumed that locking chamber pressure always reaches twice the system pressure or is zero during a part of the locked phase, the maximum of errors in movement occurs at maximum locking chamber volume.



For the DEHA studied, accordingly, maximum total displacement is about 0.56 mm (see Fig. 14, upper part). Due to the inertial action of the pistons, locking chamber pressure can also rise above twice system pressure. As can be seen in the lower part of Fig. 14, we then obtain a total displacement of 0.78 mm. In normal DEHA operation, however, this maximum movement error will not be reached because of the signal structure. The magnitude of the excess movements or movements in the wrong direction which are executed by the output piston during the locked phase is a function of signal-word changes in opposite directions and of the differences in piston travel times. In the DEHA prototype, a maximum movement error of about 0.4 mm was measured with the locking valve but without calibrated orifices during changeover from position 255 to position 256 (see Figs. 15 and 16). The effectiveness of the locking valve is again demonstrated in these plots.

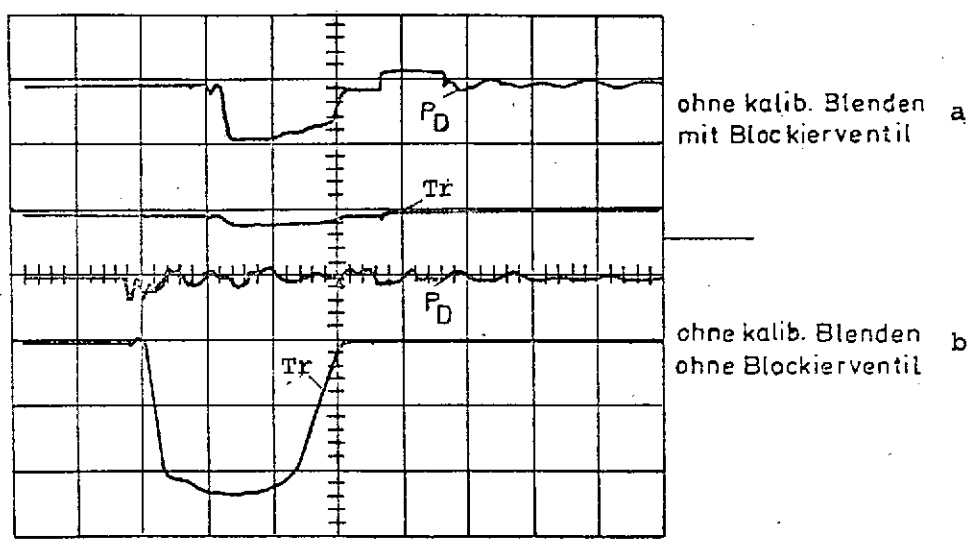


Fig. 15. Resultant movement  $Tr$  of the DEHA output piston during position change from 255 to 256.

Key: a. Without calibrated orifices, with locking valve  
 b. Without calibrated orifices, without locking valve.

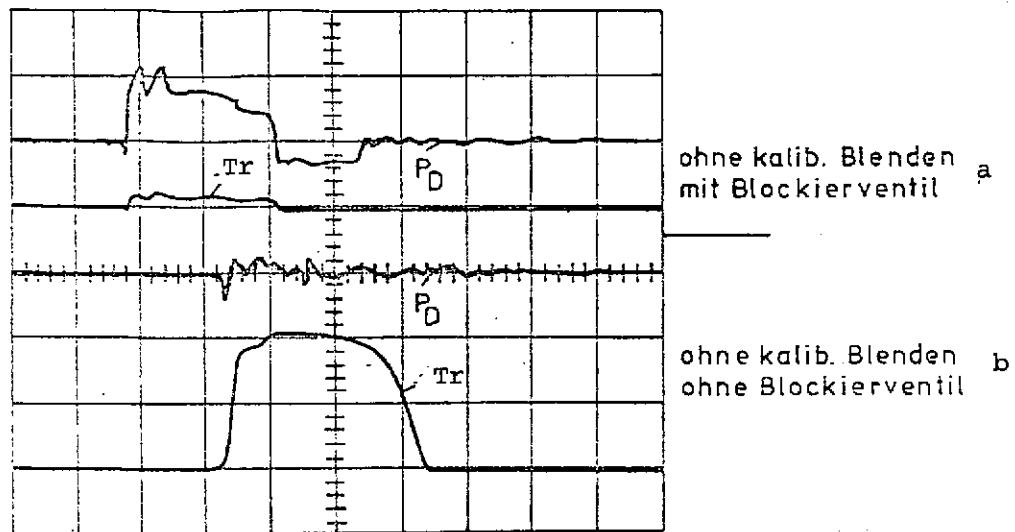


Fig. 16. Resultant movement  $Tr$  of the DEHA output piston during position change from 256 to 255.

Time scale	10 ms/Div.
Travel scale	2.5 mm/Div.
Pressure scale	98 bar/Div.
System pressure	98 bar

Key: a. Without calibrated orifices, with locking valve;  
 b. Without calibrated orifices, without locking valve

#### 4. The DEHA As an Anticipatory Control Actuator

It can be seen from the experimental results in the last section that even when a locking mechanism is used, movement errors (detrimental movements) occur in the dynamic operation of the DEHA which are not permissible, on this order of magnitude, for many types of application. Since the movement errors are of a high frequency nature -- in comparison to the square-wave frequency of the actuator -- the output piston's excess movements or movements in the wrong direction can be suppressed by the introduction of a low pass filter. A low pass filter can be

provided by means of a power amplifier which follows the DEHA. The DEHA then serves merely as an anticipatory control instrument (reference element) (see Fig. 17).

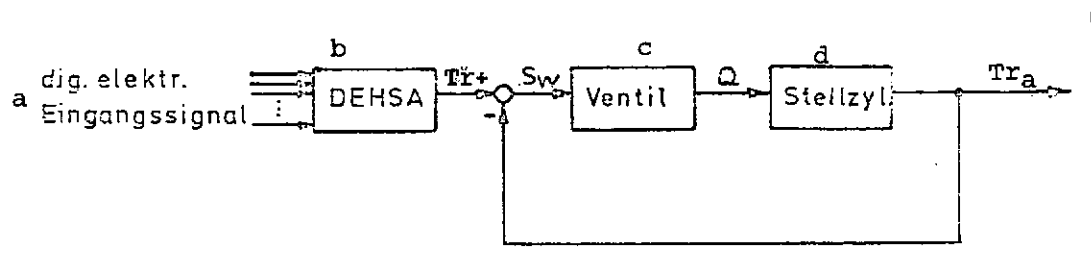


Fig. 17. Schematic of an actuator consisting of a DEHA followed by a power amplifier.

Key: a. Digital electronic input signal  
 b. DEHA  
 c. Valve  
 d. Actuator cylinder

In the tests, an aileron actuator from the Sabre MK VI (F86) was used as the power amplifier (see Fig. 19).

#### Technical Data on the Power Amplifier

Servo actuator based on the follow-up principle. Consists of a fixed tandem cylinder and a twin plunger-type valve mounted on the piston rod (see Fig. 18).

Supply pressure $P_s$	98 bar
Usable piston area $A_p - A_R$	12.8 cm <sup>2</sup>
Operating travel $Tr_a$	37 mm
Valve input signal	$\pm 1.3$ mm
Valve amplification	$Q_{max}/S_{Wmax}$ 4.5 mm <sup>3</sup> /mm·sec
Back-amplification $Tr/Tr_a$	1

The quantitative test results can be seen from Fig. 20. Even a movement error in the DEHA output piston of 0.4 mm is suppressed by the low-pass characteristic of the power amplifier.

/37

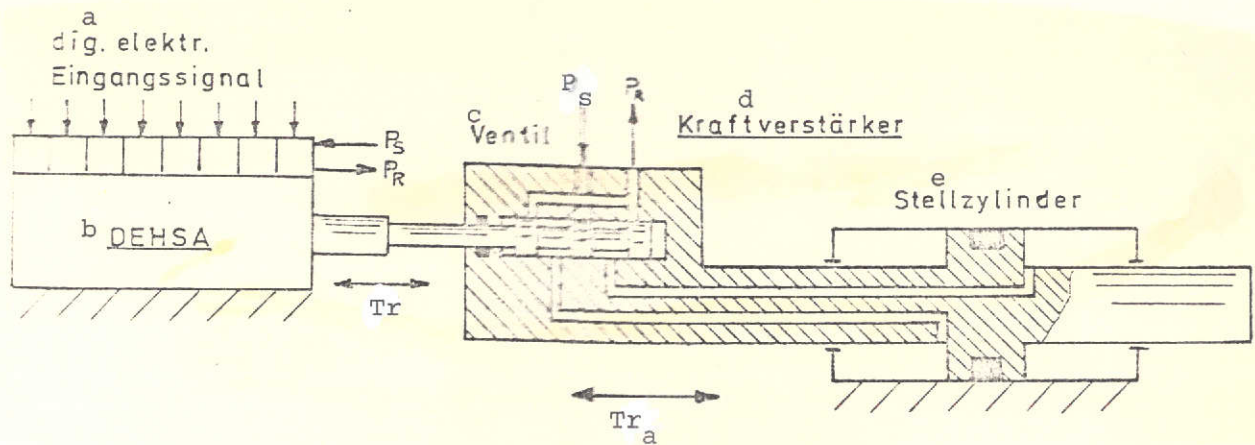


Fig. 18. Schematic of an actuator consisting of a DEHA followed by a power amplifier.

- Key:
- a. Digital electronic input signal
  - b. DEHA
  - c. Valve
  - d. Power amplifier
  - e. Actuator cylinder

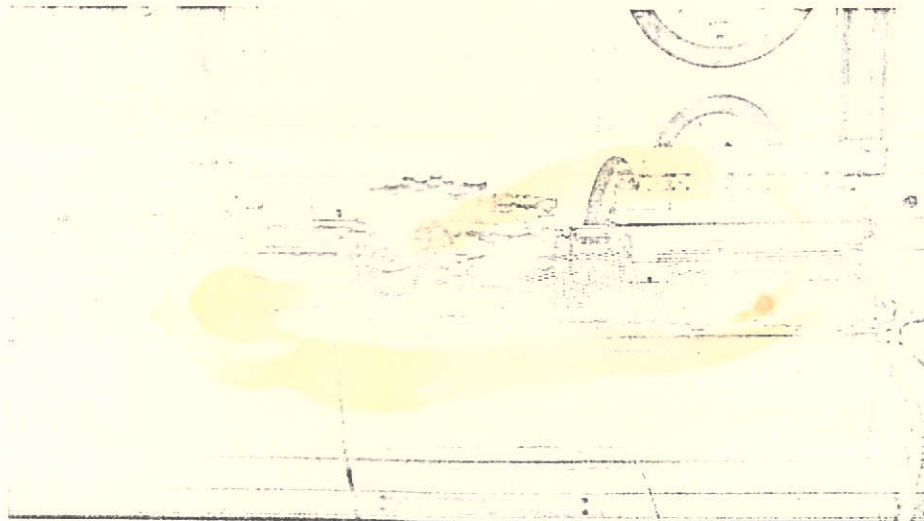


Fig. 19. Test design of the actuator, consisting of a DEHA followed by a power amplifier.

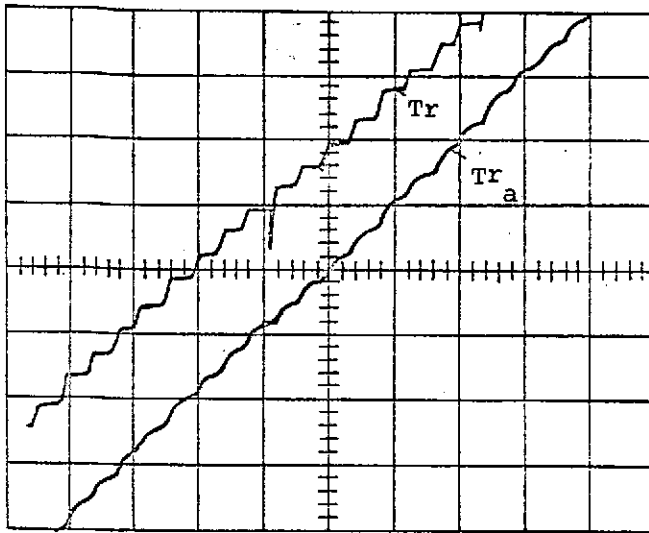


Fig. 20. Resultant movement  $Tr$  of the DEHA output piston and curve of output variable  $Tr_a$  of the power amplifier.

Time scale	1 s/Div.
Frequency	0.01 Hz
Step width	0.2 mm
Cycle frequency	20 Hz
System pressure	98 bar

The suitability of a DEHA as an anticipatory control instrument was merely meant to be demonstrated with this experiment. Generally valid statements can of course not be derived from these experimental results. In order to obtain satisfactory results in using a DEHA as an anticipatory control instrument, it is necessary to adapt the dynamic behavior of the power amplifier to that of the DEHA, i.e., since the dynamic behavior of the power amplifier is deter-

mined by the timewise behavior of the aircraft, for example, it is necessary to appropriately match the positioning velocity of the DEHA.

## 5. Summary

/38

The basic feasibility of a digital electrohydraulic actuator has been demonstrated with the construction of a prototype.

Implementation of this project required the development of electrohydraulic 3/2-way valves of high reliability and extremely short operating times. Through the use of a fluidically controlled ball switching element which was of a type that is new in hydraulics, it was possible to design the two-stage valves

with ball elements, only, thereby avoiding any plunger elements with a sealing function. The introduction of an hydraulic position memory satisfied requirements for the use of low-power pulsed triggering.

Satisfactory dynamic behavior on the part of the digital actuator is primarily determined by the accuracy of binary through-flow weighting. Since the high outlay involved in a provision for regulating through-flow results in a reduction in reliability, an attempt was made to achieve a constant oil flow with calibrated orifices only. The results obtained are still not satisfactory. Particularly high requirements are placed on measurement techniques here. The required precision can probably be achieved if production-engineering and measurement possibilities are exhausted. The long-term constancy of through-flow weighting still remains to be studied.

The required tolerance in individual piston travel could not be satisfied in producing the actuator cylinder. These problems can probably be eliminated with the experience obtained in building the prototype.

Detrimental movements (excess movements or movements in the wrong direction) due to inaccurate through-flow weighting or under loads should be avoidable if the output piston is locked until opposed low-level piston movements have been completed. The experimental results show, however, that absolute locking with a locking valve is not possible. Measurements performed on the prototype yielded maximum movement errors of about 1% of total travel. The digital actuator can thus be employed even under loads if this error is accepted. See [2] regarding restrictions under inertial loads. Relatively large weighting errors are compensated for, to the level indicated, by means of locking.

The high-frequency detrimental movements of the digital actuator are filtered out when it is used as an anticipatory control instrument for a power amplifier to which it is connected. If the timewise behaviors of the digital actuator and power amplifier are tuned to one another, their overall operation exhibits satisfactory dynamic behavior.

/39